Cell

# Encoding and Transducing the Synaptic or Extrasynaptic Origin of NMDA Receptor Signals to the Nucleus

Anna Karpova,[1,7] Marina Mikhaylova,[1,4,7] Sujoy Bera,[1] Julia Bär,[1] Pasham Parameshwar Reddy,[1] Thomas Behnisch,[5] Vladan Rankovic,[1] Christina Spilker,[1] Philipp Bethge,[1,8] Jale Sahin,[1,9] Rahul Kaushik,[1] Werner Zuschratter,[2] Thilo Kähne,[6] Michael Naumann,[6] Eckart D. Gundelfinger,[3] and Michael R. Kreutz[1,*]

[1]RG Neuroplasticity

[2]Special Lab Electron and Laserscanning Microscopy

[3]Department of Neurochemistry and Molecular Biology

Leibniz Institute for Neurobiology, 39118 Magdeburg, Germany

[4]Cell Biology, Faculty of Science, Utrecht University, 3584 CH Utrecht, the Netherlands

[5]Institutes of Brain Science and State Key Laboratory of Medical Neurobiology, Fudan University, Shanghai 200032, People's Republic of China

[6]Institute of Experimental Internal Medicine, Otto-von-Guericke University Magdeburg, 39120 Magdeburg, Germany

[7]These authors contributed equally to this work

[8]Present address: CNRS, Interdisciplinary Institute for Neuroscience, UMR 5297, 33000 Bordeaux, France

[9]Present address: National Metrology Institute, TÜBITAK-UME, 41470 PK 54 Kocaeli, Turkey

*Correspondence: kreutz@lin-magdeburg.de

http://dx.doi.org/10.1016/j.cell.2013.02.002

## SUMMARY

The activation of N-methyl-D-aspartate-receptors (NMDARs) in synapses provides plasticity and cell survival signals, whereas NMDARs residing in the neuronal membrane outside synapses trigger neurodegeneration. At present, it is unclear how these opposing signals are transduced to and discriminated by the nucleus. In this study, we demonstrate that Jacob is a protein messenger that encodes the origin of synaptic versus extrasynaptic NMDAR signals and delivers them to the nucleus. Exclusively synaptic, but not extrasynaptic, NMDAR activation induces phosphorylation of Jacob at serine-180 by ERK1/2. Long-distance trafficking of Jacob from synaptic, but not extrasynaptic, sites depends on ERK activity, and association with fragments of the intermediate filament α-internexin hinders dephosphorylation of the Jacob/ERK complex during nuclear transit. In the nucleus, the phosphorylation state of Jacob determines whether it induces cell death or promotes cell survival and enhances synaptic plasticity.

## INTRODUCTION

N-methyl-D-aspartate-receptors (NMDARs) are heterotetrameric ligand- and voltage-gated $Na^+/Ca^{2+}$ channels that play a pivotal role in synaptic plasticity and memory formation, as well as in cell death and survival signaling (Köhr, 2006; Hardingham and Bading, 2010). Many aspects of these diverse functions require the regulation of gene expression and, hence, synapse-to-nucleus communication. Thus, it is generally believed that synaptic activity regulates gene expression that is required for long-term changes of membrane excitability and the formation of long-term memory; the contribution of long-distance NMDAR signaling to the nucleus is essential in this regard (Alberini, 2009; Flavell and Greenberg, 2008; Jordan and Kreutz, 2009). However, NMDARs are present at synaptic and extrasynaptic sites. In recent years, it became increasingly clear that, depending upon their localization, the activation of these receptors has fundamentally different consequences with respect to nuclear gene expression (Hardingham and Bading, 2010). Whereas activation of synaptic NMDARs induces the expression of cell survival and plasticity genes, the activation of extrasynaptic NMDARs primarily drives the expression of cell death genes (Papadia et al., 2008; Zhang et al., 2007; Hardingham and Bading, 2010). The functional dichotomy of NMDAR signaling has attracted enormous interest as the extrasynaptic pathway was linked to disease states like brain ischemia, Huntington's disease, and others (Okamoto et al., 2009; Milnerwood et al., 2010; Tu et al., 2010; Zhang et al., 2011). To date, no molecular mechanisms are known that couple long-distance synaptic and extrasynaptic NMDAR signaling to gene expression or that distinguish both pathways in the nucleus (Hardingham and Bading, 2010).

Previously, we found that extrasynaptic NMDAR activation, as well as pathogenic agents (e.g., amyloid-β peptide), induces long-haul transport of the protein messenger Jacob to the nucleus, where it then induces a sustained dephosphorylation of CREB, rendering the transcription factor inactive (Dieterich et al., 2008; Rönicke et al., 2011). Overexpression of Jacob results in gene expression that elicits neurodegeneration, whereas suppression has the opposite effect (Dieterich et al.,

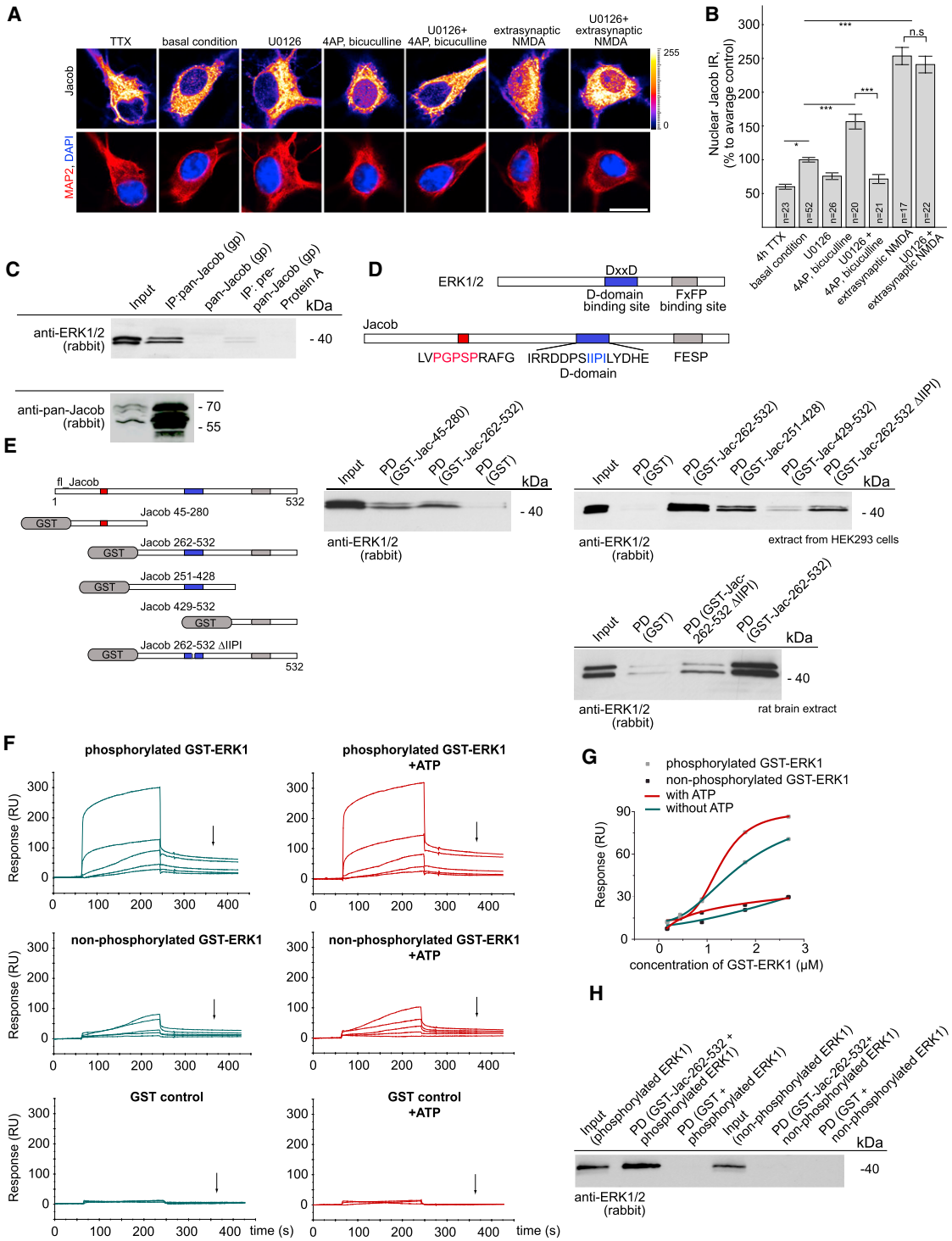


**Figure 1. The Nuclear Translocation of Jacob after Activation of Synaptic NMDARs, but Not Extrasynaptic NMDARs, Requires MAP Kinase Activity and Physical Interaction of Jacob with ERK1/2**

(A and B) The increase in nuclear Jacob immunoreactivity after enhanced synaptic NMDAR activity is accompanied by a higher activation level of ERK. Nuclear import of Jacob is abolished by application of the MEK inhibitor U0126 (10 μM). The presence of MEK inhibitor during extrasynaptic NMDAR stimulation does not prevent the nuclear import of Jacob. Confocal images averaged from three confocal sections of the nucleus of DIV16 hippocampal primary neurons stained for pan-Jacob (rabbit) and for the active form of ERK1/2 (pERK, mouse). Original pixel intensities from 0 to 255 are represented as a gradient lookup table. Scale bar, 10 μm. Intensity-based quantification of nuclear Jacob IR. Data are represented as mean ±SEM. ***p < 0.001, as determined by Bonferroni corrected t tests.

*(legend continued on next page)*

2008). Taken together, these data suggest that Jacob is a messenger of cell death in the extrasynaptic NMDAR pathway to the nucleus (Dieterich et al., 2008; Kindler et al., 2009; Rönicke et al., 2011).

However, the protein also translocates to the nucleus after stimulation of synaptic NMDARs, albeit to a lesser extent (Dieterich et al., 2008), as well as after the induction of NMDAR-dependent long-term potentiation (LTP), but not long-term depression (LTD), in CA1 neurons, suggesting that Jacob might also be involved in hippocampal LTP-dependent learning and memory processes (Behnisch et al., 2011). Given that Jacob is a messenger in both pathways, the following questions arise: how is it possible to distinguish whether the activation of extrasynaptic or synaptic NMDARs caused its nuclear import and why does this occur after the induction of NMDAR-dependent LTP, but not LTD?

Activation of the mitogen-activated protein kinase (MAPK) ERK1/2 in the hippocampus requires high-frequency stimulation of NMDARs. The induction of LTP, but not LTD, results in ERK1/2 phosphorylation (Thomas and Huganir, 2004). Most importantly, extrasynaptic NMDAR signaling has no effect on ERK1/2 phosphorylation, whereas sustained synaptic NMDAR signaling triggers the nuclear import of active ERK1/2 (Ivanov et al., 2006; Kim et al., 2005; Hardingham and Bading, 2010). Here, we show that, after sustained stimulation of synaptic NMDARs, but not of extrasynaptic NMDARs, the nuclear translocation of Jacob becomes dependent on ERK1/2 activity. Moreover, we demonstrate that Jacob is an ERK-binding protein that is phosphorylated by ERK1 at serine 180 after enhanced activation of synaptic NMDARs. Binding of the neurofilament $\alpha$-internexin forms a stable trimeric complex that hinders the dephosphorylation of Jacob and ERK during long-distance transport. We show that NMDAR-dependent LTP, but not LTD, increases Ser180 phosphorylation and that the nuclear overexpression of a phosphomimetic Jacob mutant leads to gene expression and subsequent morphological and electrophysiological changes characteristic of enhanced synaptic strength. The presence of nonphosphorylated Jacob in the nucleus has the opposite effect and is followed by a series of deteriorative events in terms of synaptic integrity that subsequently cause cell death. In summary, Ser180 phosphorylation of Jacob by ERK encodes the synaptic versus extrasynaptic localization of NMDARs, thus providing the first mechanism to distinguish these pathways in the nucleus.

## RESULTS

### ERK Activity Distinguishes the Synaptic and Extrasynaptic NMDAR-Jacob Pathways

The MAP kinase ERK1/2 are downstream effectors of synaptic NMDARs involved in NMDAR-activation-induced gene expression, whereas signaling via extrasynaptic NMDAR has no effect on ERK1/2 (Kim et al., 2005; Ivanov et al., 2006). We therefore asked whether ERK1/2 activity is required for the nuclear translocation of Jacob after synaptic NMDAR stimulation. Intriguingly, we found that U0126, a MEK1/2 inhibitor, blocks the nuclear accumulation of Jacob after selective stimulation of synaptic NMDARs, but not of extrasynaptic NMDARs (Figures 1A and 1B).

### Jacob Directly Associates with ERK and Is an ERK Substrate

Coimmunoprecipitation experiments confirmed that Jacob and ERK1/2 form a complex in vivo (Figure 1C). Jacob harbors a potential ERK phosphorylation site at serine 180 and has two potential ERK-binding domains at amino acids 367–382 and 487–501 (Figure 1D and Figure S1A available online). To learn how Jacob associates with ERK, we performed pull-down assays using recombinant GST-Jacob and HEK293 cell or rat brain extracts. In these experiments, endogenous ERK1/2 were pulled down with both the N- and C-terminal halves of Jacob (Figure 1E). Binding was much weaker to a fusion protein lacking four amino acids in the first ERK-binding domain (Jacob-ΔIIPI lacking the D domain) or to a fusion protein harboring only the FESP motif (Figures 1D and 1E), suggesting that the D domain might have the highest affinity for binding.

We next analyzed the interaction in quantitative terms employing surface plasmon resonance (SPR). We coupled recombinant 6xHis-SUMO-Jacob-Δ1-44 to the surface of a sensor chip and injected phosphorylated and nonphosphorylated GST-ERK1 fusion proteins. Although a GST-control protein did not bind to

(C) Coimmunoprecipitation of Jacob and ERK1/2 from a soluble rat brain protein fraction. Immunoprecipitation (IP) with a pan-Jacob guinea pig antibody. Two bands are visible in the precipitate that correspond to ERK1 and 2. ERK1/2 were only found in the IP with the Jacob antibody, whereas they remained in the supernatant of a preimmune serum IgG, a pan-Jacob antibody IP control without brain extract, and a Protein A sepharose control. Lower panel shows the efficiency of immunoprecipitation.

(D) Two predicted docking sites at the C terminus of Jacob identified by sequence homology to other ERK1/2 substrate binding motifs (D domain, blue box; FXFP docking site, gray box).

(E) Cartoon depicting GST-Jacob constructs used for the pull-down assays. Both the N and C termini of Jacob bind to ERK1/2 from HEK293 cell extracts in GST pull-down assay (middle). Deletion of the IIPI motif (D domain) reduces Jacob-ERK1/2 binding (right). A weak interaction was observed between ERK and the C terminus of Jacob that contains only the FxSP motif (right). Similar results were obtained in pull-down assays using a rat brain extract (bottom).

(F) SPR studies confirm the direct interaction between 6xHis-SUMO-Jacob-Δ1-44 and ERK1. The presence of ATP in the analyte enhances binding of phosphorylated ERK1 to Jacob. 6xHis-SUMO-Jacob-Δ1-44 was immobilized on the sensor chip, and phosphorylated GST-ERK1, nonphosphorylated GST-ERK1, and GST controls were added as analyte. Assays were carried out in the presence or absence of adenosine triphosphate ($Mg^{2+}$-ATP; 30 μM). Sensorgrams were processed by blank subtraction showing the net increase in amplitudes. Maximal response units in the dissociation phase for different concentrations were plotted (indicated by an arrow) and used to compare different conditions.

(G) Saturation of binding plotted from the dissociation phase of the interaction indicates higher affinity binding for phosphorylated ERK1 as compared to the nonphosphorylated kinase.

(H) GST pull-down assays using bacterially expressed GST-Jacob-262-532 and recombinant ERK1. The matrix-coupled GST-Jacob fusion protein efficiently pulls down phosphorylated ERK1, but not nonphosphorylated ERK1.

See also Figure S1.

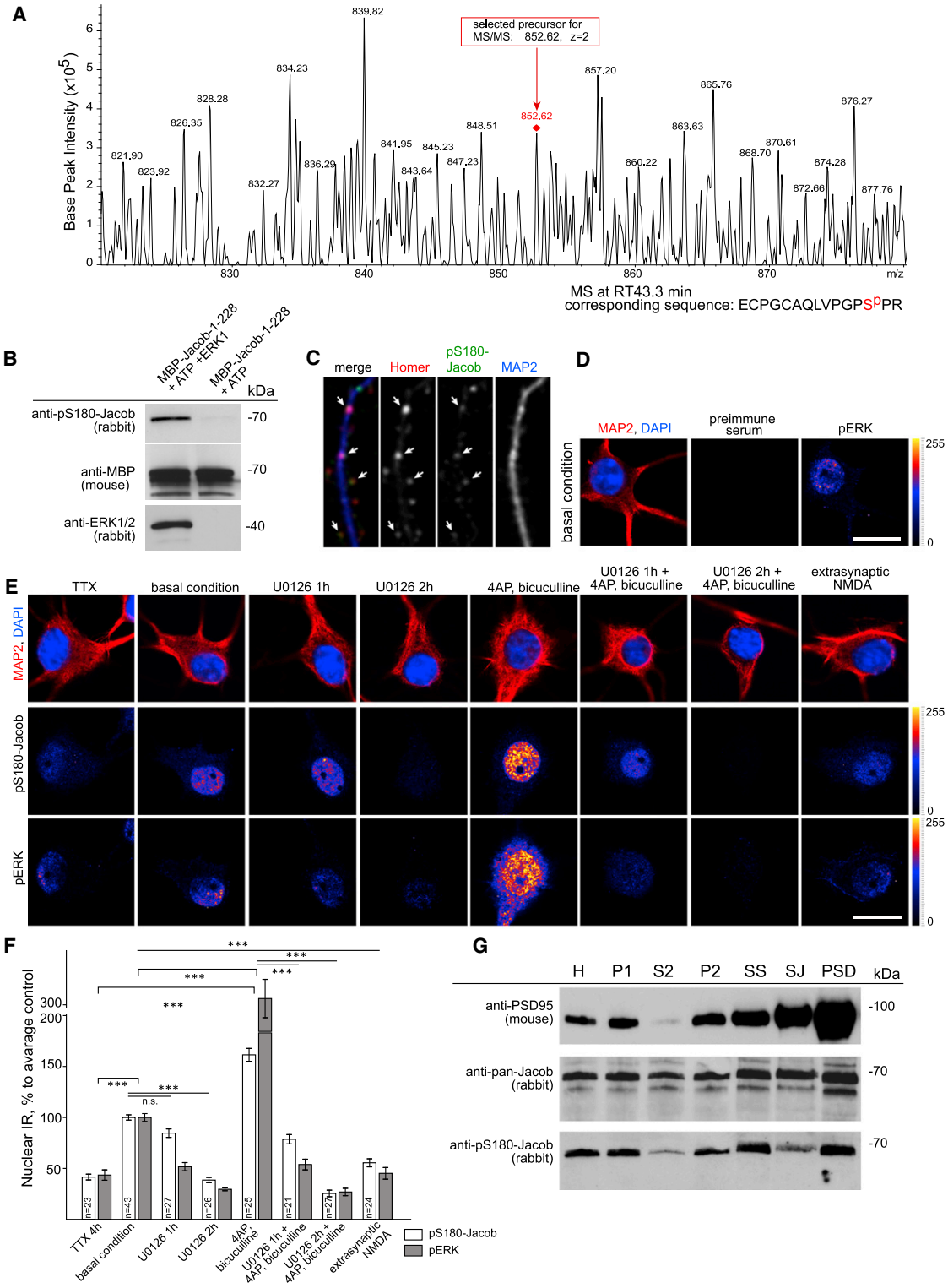


**Figure 2. Jacob Is an ERK1 Substrate In Vitro and In Vivo**

(A) ERK phosphorylates Jacob in 18DIV cortical primary neurons treated with 50 μM bicuculline/2.5 mM 4-AP. Nuclear extracts from WT-Jacob-GFP-infected neurons were separated in duplicate by SDS-PAGE. One lane from each sample was processed for immunoblotting with GFP and pS180-Jacob antibody, and a second one was stained with Coomassie blue. The area corresponding to the band of WT-Jacob-GFP was cut out from the SDS gel and underwent InGel digestion. Resulting peptides were subjected to a nanoreversed phase (C18)-HPLC online coupled to an ETDII iontrap mass spectrometer. Tandem mass

*(legend continued on next page)*

immobilized Jacob, we found a specific and saturable binding of GST-ERK1 (Figure 1F). Moreover, we observed that binding to Jacob is dependent upon ERK activity. Nonphosphorylated ERK1 associated to a much lower extent than phosphorylated ERK1, as determined from the dissociation phase of the interaction (Figures 1F and 1G). A further increase in response was seen when we added ATP, conditions which promote the phosphorylation of Jacob by ERK1 (Figure 1F). In addition, a GST-Jacob fusion protein interacts more efficiently with active versus inactive ERK1 (Figure 1H).

Next, we directly assessed whether Ser180 is an ERK phosphorylation site. An in vitro ERK kinase assay and subsequent nano-LC-ESI-MS/MS analysis demonstrated the incorporation of a phosphate at position 180 in a bacterially expressed 6-His-SUMO-Jacob-Δ1-44 fusion protein (Figures S1A and S2A). No other phosphorylation site was identified in this assay (Figure S2A). In addition, this phosphorylation site is highly conserved in different mammalian species (except mouse, see Supplemental Information and Figures S1B–S1F). Moreover, we found that, after viral expression of WT-Jacob-GFP in primary cortical neurons, Jacob is phosphorylated at serine 180 in vivo (Figure 2A).

## Ser180 Phosphorylation Is Induced by Synaptic Activity

To further explore the role of phosphorylation at this site, we generated a phosphospecific antibody (pS180-Jacob; see Extended Experimental Procedures and Figures 2B–2E and S2B–S2H). The antibody detects phospho-S180 in an MBP-Jacob-1-228 fusion protein preincubated with active ERK1 and ATP, but not the nonphosphorylated Jacob (Figure 2B). Immunocytochemical staining revealed prominent pS180-Jacob immunofluorescence in the nucleus and synapses and, to a lesser extent, in dendrites (Figures 2C–2E). Moreover, pS180-Jacob immunoreactivity (IR) was detected in the postsynaptic density fraction (PSD) in subcellular fractionation experiments (Figure 2G). We next asked whether synaptic and extrasynaptic NMDAR stimulation might differentially regulate the phosphorylation of Jacob. Only in the first case did we find an increased nuclear pS180-Jacob immunofluorescence, whereas extrasynaptic NMDAR stimulation had the opposite effect (Figures 2E and 2F). The increase in staining intensity was blocked when, concomitant to enhancing synaptic activity, the MEK inhibitor U0126 was applied (Figures 2E and 2F). Interestingly, nuclear overexpression of myristoylation-deficient Jacob-ΔIIPI, lacking the high-affinity ERK docking site, showed no enhancement of pS180-Jacob immunostaining as compared to the corresponding myristoylation mutant containing this binding motif (Figure S2E). Scansite 2.0 suggests that Ser180 might also be phosphorylated by cyclin-dependent kinase 5 (CDK5). However, administration of the CDK5 inhibitor roscovitine had no effect on pS180 immunofluorescence (Figures S2F–S2H), suggesting that Ser180 is most likely a specific ERK phosphorylation site in vivo.

## Jacob Translocates from Synapses to the Nucleus in an ERK-Dependent Manner

For any molecule to be considered a true synapto-nuclear messenger, a minimum requirement is an activity-dependent dissociation from synaptic sites, which correlates with an increase in nuclear protein levels. Because the latter was previously shown (Dieterich et al., 2008; Kindler et al., 2009), we increased network activity and synaptic glutamate release with bicuculline and applied quantitative immunocytochemistry to study the synaptic association of Jacob. As shown in Figure S3, the immunofluorescence of synaptic Jacob was indeed significantly reduced within 10 min following bicuculline application, as compared to tetrodotoxin (TTX)-treated control neurons (Figures S3A and S3B). Most importantly, high-frequency field stimulation (18 s/50 Hz), which induces LTP in hippocampal primary neurons (Deisseroth et al., 1996), leads to a pronounced and rapid dissociation of WT-Jacob-GFP from dendritic spines (Figures 3A and 3B). Further evidence that Jacob rapidly dissociates from synaptic sites in an activity- and ERK-dependent manner was obtained when we expressed full-length Jacob-GFP in primary neurons using a Semliki-Forest virus (Figures S3C and S3D). After stimulation of synaptic NMDARs, WT-Jacob-GFP rapidly moved out of dendritic spines (Figures S3C and S3D), whereas it was retained in dendritic spines following stimulation when we preincubated the culture with the MEK-inhibitor U0126 (Figure 3D). We then generated a phosphodeficient mutant by replacing Ser180 with alanine (S180A- Jacob-GFP). DIV25-27 neurons were transfected with WT-Jacob-GFP

spectrometry (MS/MS) precursor selection was tuned for the preferential use of masses corresponding to a double-charged (852.36 Da) putative ECPGCAQLVPGPSPPR Jacob peptide. Depicted is the mass spectrum at retention time 43.3 min, including the 852.62 Da double-charged base peak peptide, which was selected as a precursor for two independent collision-induced dissociation (CID) fragmentations. Both MS/MS experiments significantly revealed sequence identity of the selected precursor to the phosphorylated ECPGCAQLVPGPSpPR sequence of Jacob.

(B) The anti-pS180-Jacob antibody recognizes phosphorylated Jacob, but not nonphosphorylated Jacob. Recombinant active ERK1 was used to phosphorylate bacterially expressed MBP-Jacob-1-228 at Ser180 in the presence of ATP. Anti-MBP antibody staining shows that equal amounts of protein were used in both reactions.

(C) A representative confocal image of dendritic segment stained with an anti-MAP2 antibody (blue) is depicted. Arrows indicate pS180-Jacob spots at a subset of excitatory synapses as demonstrated by double-immunofluorescence staining with an anti-Homer antibody (red).

(D) The pS180 Jacob preimmune serum shows no nuclear staining. Scale bar, 20 μm.

(E and F) Enhanced synaptic activity increases nuclear pS180-Jacob IR. The increase is abolished in the presence of 10 μM U0126. In contrast, stimulation of extrasynaptic NMDARs results in a decrease of nuclear pS180-Jacob IR. Scale bar, 20 μm. Data are represented as mean ±SEM. ***$p < 0.001$, as determined by Bonferroni corrected t tests.

(G) Subcellular fractionation of rat brain. A 70 kDa pS180-Jacob band is present in the PSD fraction. Please note that Jacob is alternatively spliced, which results in multiple bands on western blots (Dieterich et al., 2008; Kindler et al., 2009). Low-molecular-weight pS180-Jacob bands are only visible at long exposure times. 20 μg of protein was loaded in each lane. H, homogenate; P1, crude nuclear fraction; S2, supernatant after centrifugation at 12,000 x *g*; P2, pellet fraction generated after centrifugation of precleaned homogenate at 12,000 x *g*; SS, synaptosomes; SJ, synaptic junctions; and PSD, postsynaptic density fraction. See also Figures S1 and S2.

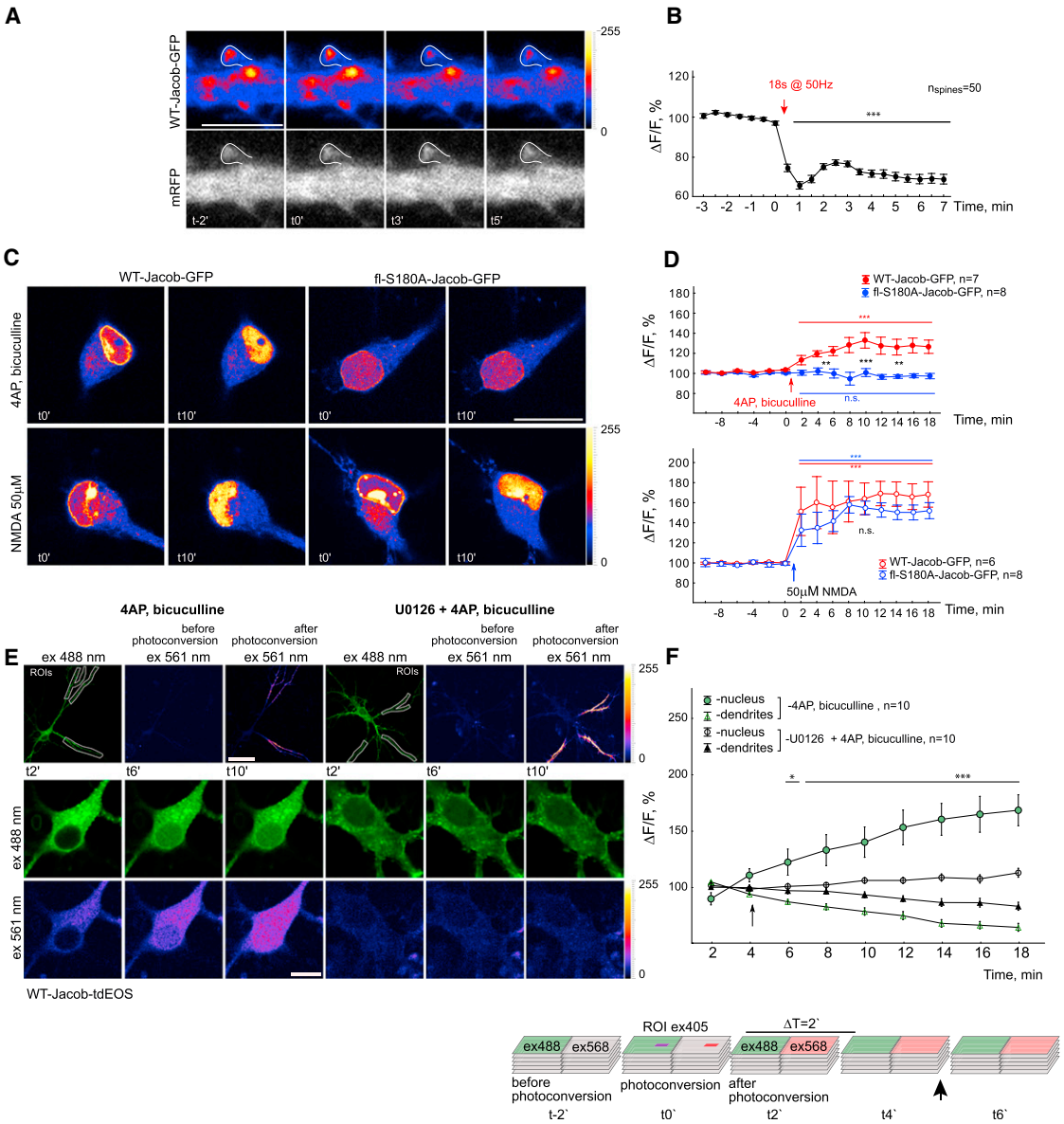


**Figure 3. Synaptic Stimulation Drives Jacob from Distal Dendrites into the Nucleus in an ERK-Dependent Manner**

(A and B) High-frequency field stimulation (50 Hz pulses for 18 s, 1 ms current pulse duration) results in a rapid and prominent dissociation of WT-Jacob-GFP from dendritic spines. Coexpression of mRFP served as a volume control. Depicted are representative confocal frames before (t-2′, t0′) and after (t3′, t5′) synaptic stimulation. Scale bar, 5 μm.

(C and D) Time-lapse imaging reveals that the translocation of Jacob from distal dendrites to the nucleus depends upon Ser180 phosphorylation following stimulation of synaptic NMDARs, but not extrasynaptic NMDARs. Confocal average intensity images of hippocampal neurons at DIV16/17 expressing WT-Jacob-GFP or Jacob-S180A-GFP are shown before (t0′) and after (t10′) stimulation. Scale bar, 25 μm. Nuclear Jacob-S180A-GFP (blue circles) and WT-Jacob-GFP (red circles) fluorescence intensities before and after 4-AP, bicuculline application or after bath application of 50 μM NMDA (open circles, bottom). Data are represented as mean ±SEM. ***$p < 0.001$, as determined by Bonferroni corrected t tests.

(E and F) Jacob-tdEOS was expressed in hippocampal primary neurons, and indicated regions of interest (ROIs) were illuminated with 405 nm wavelength to induce green-to-red fluorescence conversion in distal dendrites. The upper panels in (E) show effective photoconversion after illumination with 405 nm. Scale bar, 40 μm. The lower panels depict (35 × 35) $\mu m^2$ averaged frames from the nuclear plane before (t2′) and after (t6′ and t10′) synaptic stimulation. Scale bar, 10 μm. WT-Jacob-tdEOS photoconverted at distal dendrites translocates to the nucleus upon synaptic stimulation (green circles in F). At the same time, a decrease in tdEOS photoconverted fluorescence was observed at distal dendrites (F, green triangles). The presence of the MEK antagonist U0126 blocked this translocation. Data are represented as mean ±SEM. *$p < 0.05$ and ***$p < 0.001$. (F) Confocal z stacks were acquired using the xyzt-image scan mode with a 0.3 μm step size and ΔT = 2′. ROIs selected for photoconversion were illuminated with 405 nm light, and the out-of-ROI region was set to 488 nm excitation wavelength. The arrow at t4 indicates the time point of synaptic stimulation. Time points t2 and t4 were taken as baseline, and changes in pixel intensities upon bicuculline treatment were normalized to the averaged baseline.

See also Figure S3.

or the S180A mutant (Figures S3E and S3F). As expected, and in contrast to wild-type, S180A- Jacob-GFP remained at synaptic sites following enhanced synaptic NMDAR activity (Figures S3E and S3F).

We next asked whether the long-distance trafficking of Jacob to the nucleus after synaptic NMDAR activation depends upon the phosphorylation of Ser180 by ERK. Time-lapse imaging of hippocampal neurons transfected with the phosphodeficient Jacob-GFP mutant revealed that this fusion protein only accumulates in the nucleus after the activation of extrasynaptic (Figures 3C and 3D, bottom), but not synaptic, NMDARs following administration of 4-AP and bicuculline (Figures 3C and 3D, top). Further evidence for ERK-dependent Ser180 phosphorylation as a prerequisite for long-distance trafficking in response to synaptic NMDAR stimulation came from experiments where we transfected primary hippocampal neurons with a photoconvertible WT-Jacob-tdEos construct that allows the conversion of green to red fluorescence in more distal dendrites, including spines (Figures 3E and 3F). Following bath application of bicuculline, we observed a rapid increase in the nuclear red fluorescence signal within minutes, indicating dendrite-to-nucleus trafficking (Figures 3E and 3F). In stark contrast, the WT-Jacob-tdEos fusion protein remained largely stationary in dendrites when we repeated this experiment in the presence of the MEK inhibitor U0126 (Figures 3E and 3F), indicating that Ser180 phosphorylation and ERK activity are indeed necessary for long-distance synapse to nucleus trafficking.

### Binding to α-Internexin Protects Phosphorylated Jacob against Phosphatase Activity during Long-Distance Trafficking to the Nucleus

Taken together, these results raise the question of whether it is at all conceivable that Jacob can traverse a phosphatase-rich environment and preserve its phosphorylation status for long-distance synapto-nuclear signaling. A plausible mechanism for the conservation of posttranslational modifications for long-distance transport was suggested by Perlson et al. (2005), who demonstrated that retrograde transport of ERK1/2 in axons requires association with importin-β and the molecular motor dynein. The concomitant binding of proteolytic fragments of the intermediate filament vimentin hinders the dephosphorylation of pERK within this complex (Perlson et al., 2005, 2006). In a yeast two-hybrid screen with Jacob, we identified α-internexin as a binding partner (Figure S4A). α-Internexin is a neuronal intermediate filament and, in contrast to vimentin, is expressed in adult neurons where it replaces vimentin during neuronal development (Benson et al., 1996; Yuan et al., 2006). We found that α-internexin is present in different subcellular fractions from adult rat brain homogenates, including cytosol, nuclei, and the PSD (Figures 4A and S5A). Immunocytochemistry revealed staining in neurites, somata, and nuclei (Figures S4B, S4C, and S5B), whereas only a sparse α-internexin staining was present in dendritic spines (Figure S4B). Analogous to vimentin, we found that α-internexin is also sensitive to proteolytic cleavage by the calcium-activated protease calpain (Figure S5C).

A GST pull-down assay using recombinant full-length α-internexin and cell extracts from HEK293 cells transfected with c-*myc*-tagged Jacob confirmed the interaction between both proteins (Figure S4D). The reciprocal pull-down with GST Jac-45-280 shows binding of α-internexin from rat brain extract (Figure S4D). Neuronal importins are present in axons, dendrites, and at synapses from where they translocate to the nucleus upon NMDAR activation (Thompson et al., 2004). Importin-α can directly associate with a dynein motor (Hanz et al., 2003), and we have previously shown that long-distance transport of Jacob requires importin-α binding (Dieterich et al., 2008), suggesting that an active transport along microtubuli is responsible for the activity-dependent nuclear import of Jacob. In support of this notion, Jacob, α-internexin, ERK1/2, importin-α, and the dynein intermediate chain are all present in a soluble microsome-free cytoplasmic fraction. Additionally, α-internexin could be coimmunoprecipitated with an anti-dynein intermediate chain antibody (Figures 4A and 4B), indicating that these proteins may associate in one complex in vivo. We next mapped the binding regions of the Jacob/α-internexin interaction using the yeast two-hybrid system. We found that an N- and C-terminal binding site exists in Jacob for the interaction with α-internexin (Figure S4A). The N-terminal site encompasses Ser180, and GST-α-internexin pulled down Jacob more efficiently after enhanced ERK activity (Figure S4E). Stimulation of HEK293 cells with EGF to increase MAPK activity enhanced binding of Jacob, whereas application of the MEK inhibitor U0126 had the opposite effect (Figure S4E). Furthermore, a direct interaction between Jacob and α-internexin was confirmed with GST pull-down assays using the recombinant proteins (Figure S4G). However, no interaction was found between GST-ERK1/2 and α-internexin (Figure S4F). Finally, binding of α-internexin does not compete with ERK binding nor does it prevent phosphorylation of Jacob by ERK in in vitro kinase assays (Figures S4G and S4H).

We next asked whether the binding of α-internexin might protect Jacob from dephosphorylation. To address this question, we incubated recombinant MBP-Jacob and pERK1 in the presence or absence of α-internexin fusion proteins of different lengths with mouse brain extracts lacking phosphatase inhibitors. We found that the dephosphorylation of both pJacob and pERK1 was attenuated for periods up to 20 min in the presence of fusion proteins containing C-terminal fragments of α-internexin (Figure 4C). However, when we repeated this assay after disassembly of the protein complex with gel electrophoresis and subsequently incubated the membranes with GST fusion constructs of α-internexin and mouse brain extracts, immunoblotting with anti-pS180-Jacob and anti-pERK1/2 revealed that α-internexin only prevents the dephosphorylation of pJacob, but not of pERK1 (Figure 4D). Taken together, these data point to a scenario in which synaptic NMDARs activate ERK, which then binds and phosphorylates Jacob. This, in turn, enhances the binding of Jacob to a C-terminal fragment of α-internexin, which then prevents dephosphorylation of Jacob and pERK bound to Jacob. The trimeric complex appears to be quite stable and thus well suited for long-distance transport. Indeed, we observed an accumulation of nuclear α-internexin immunofluorescence following enhanced activity of synaptic NMDARs (Figure S5B). Finally, experiments where we knocked down α-internexin with shRNA showed that α-internexin probably stabilizes a transport complex for synapse-to-nucleus

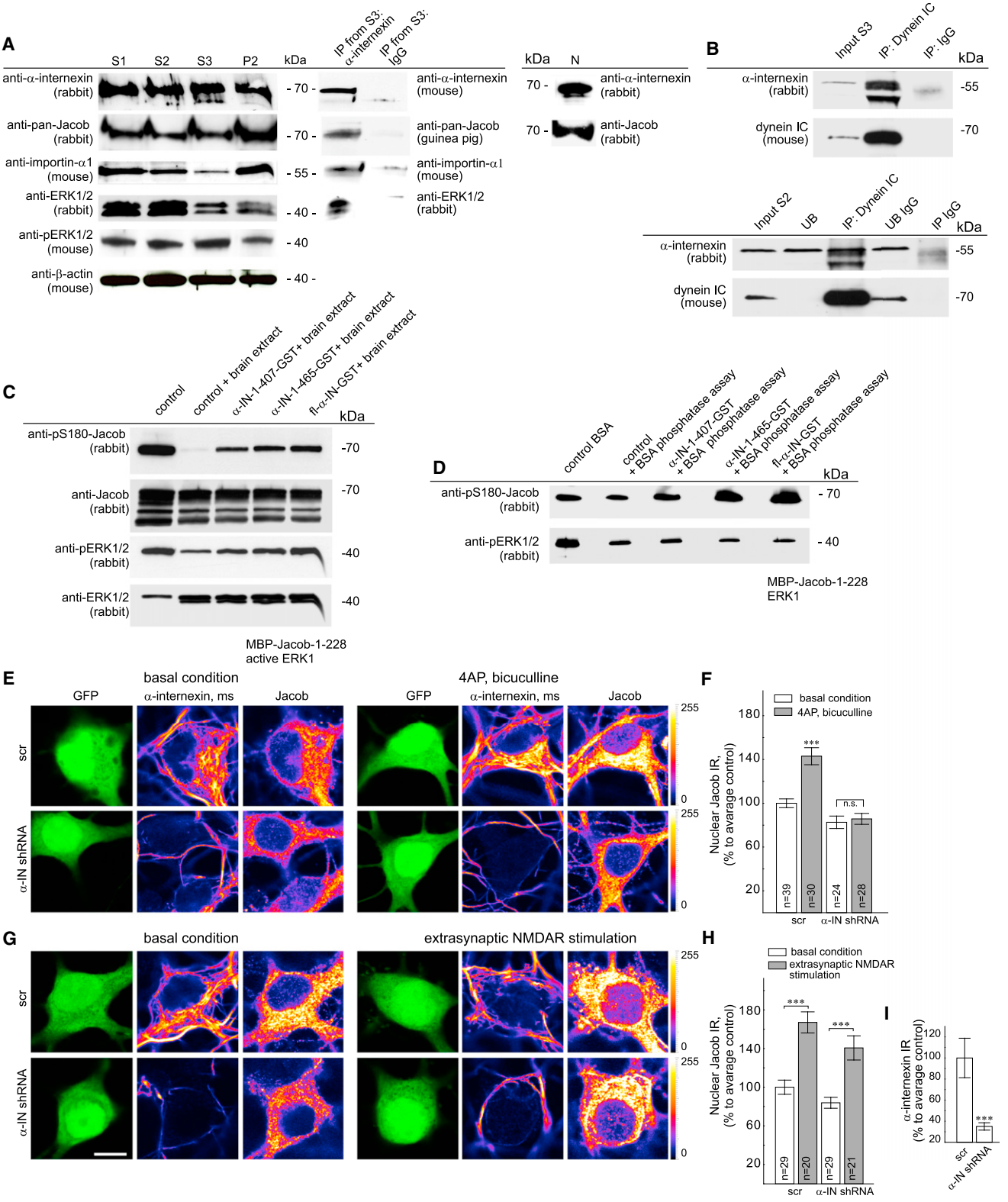


**Figure 4. Binding of α-Internexin Protects Jacob against Phosphatase Activity and Is Involved in Nuclear Transit of Jacob upon Enhanced Synaptic Activity**

(A) Immunoblotting of Jacob, importin-α1, α-internexin, and ERK in subcellular fractions from adult rat brain. 7 μg of protein was loaded in each lane. S1, pre-cleaned homogenate after centrifugation at 1,000 x *g*; S2, supernatant after removal of mitochondria and heavy membranes by centrifugation at 12,000 x *g*, S3,

*(legend continued on next page)*

signaling (Figures 4E–4H). In neurons with significantly lower α-internexin levels, the nuclear import of Jacob was significantly reduced after stimulation of synaptic NMDARs (Figures 4G and 4H), but not extrasynaptic NMDARs (Figures 4H and 4I).

### pS180-Jacob Accumulates in the Nucleus following the Induction of LTP

We have previously reported that Jacob translocates to the nucleus following the induction of NMDAR-dependent LTP, but not LTD (Behnisch et al., 2011). We found that the induction of chemical LTP was also accompanied by an increase in nuclear pS180-Jacob immunofluorescence, whereas the induction of chemical LTD had the opposite effect (Figures 5A and 5B). To substantiate this finding, we induced and measured the induction of Schaffer collateral LTP in acute brain slices and subsequently isolated neuronal nuclei from CA1 neurons. We first showed that the most prominent pS180 Jacob band in hippocampal CA1 homogenates is not present on immunoblots if the samples are processed in the absence of phosphatase inhibitors (Figure 5C), showing that the antibody does not detect nonphosphorylated endogenous Jacob. We then applied high-frequency stimulation and monitored the induction of LTP for each slice that was subsequently processed for immunoblotting (Figure 5D). Quantitative immunoblotting revealed that, 2 and 30 min following the induction of LTP, pS180 Jacob levels remained unaltered in total CA1 protein homogenates (Figures 5E and 5F), which is not surprising because only a subset of cells will be tetanized. Also, no change in pS180 Jacob levels was observed in nuclear-enriched fractions 2 min after tetanization (Figures 5E and 5F), a time point at which Jacob levels just start to increase in the nucleus following LTP induction (Behnisch et al., 2011). However, we found a 2-fold increase in pS180-Jacob immunoreactivity 30 min after tetanization (Figures 5E and 5F), a time point at which Jacob levels peak in the nucleus (Behnisch et al., 2011). Immunofluorescence stainings confirmed the LTP-induced increase of pS180-Jacob immunoreactivity in nuclei of CA1 neurons (Figure 5G). Thus, Jacob that translocates to the nucleus in a cellular model of learning and memory is phosphorylated at Ser180.

### Phosphomimetic and Phosphodeficient Jacob Have Opposite Effects on CREB "Shut-Off," Gene Expression, Cell Survival, and Synaptic Activity

Finally, we asked whether ERK phosphorylation prior to the nuclear entry of Jacob has functional consequences in terms of gene expression, cellular integrity, and synaptic activity. We first investigated whether Ser180 phosphorylation affects the phosphorylation of CREB. N-terminal myristoylation of Jacob is essential for its extranuclear localization (Dieterich et al., 2008). An N-terminal fragment has to be cleaved by calpain before nuclear transit can occur (Kindler et al., 2009). We generated a myristoylation-deficient phosphomimetic mutant, ΔMyr-S180D-Jacob-GFP, that accumulates in the nucleus by default (Figure 6A). Overexpression of ΔMyr-S180D-Jacob-GFP in primary neurons led to a significantly increased pCREB immunofluorescence in the nucleus (Figures 6A, top, and 6B), whereas transfection with the corresponding phosphodeficient mutant ΔMyr-S180A-Jacob-GFP had the opposite effect (Figures 6A and 6B). Interestingly, the increase in pCREB immunofluorescence after nuclear overexpression of phosphomimetic Jacob was also seen in cultures that were silenced by application of TTX, NBQX, and APV (Figures S6A and S6B). Nuclear overexpression of ΔMyr-Jacob leads to CREB shut-off, a drastic simplification of synapto-dendritic complexity, and subsequent cellular degeneration (Dieterich et al., 2008) despite the fact that it can be phosphorylated by ERK. We therefore addressed the question of whether enhanced synaptic activity and the resulting nuclear import of active ERK and subsequent phosphorylation of nuclear ΔMyr-Jacob-GFP (Figures S2E and S2F) might prevent the cellular degeneration seen with this construct. In cultures that were kept in the presence of bicuculline and 4-AP following transfection, enhanced ERK activity was indeed accompanied by increased nuclear pCREB immunostaining in neurons overexpressing ΔMyr-Jacob-GFP (Figures 6A, bottom, and 6B). By contrast, neurons that were transfected with the phosphodeficient mutant ΔMyr-S180A-Jacob showed a CREB shut-off irrespective of the culture conditions (Figures 6A and 6B). As in our previous study (Dieterich et al., 2008), we found a reduced synapto-dendritic complexity under resting conditions in hippocampal neurons expressing either ΔMyr-Jacob-GFP or the phosphodeficient mutant ΔMyr-S180A-Jacob-GFP, but not the phosphomimetic mutant ΔMyr-S180D-Jacob-GFP (Figures 6C–6E). Enhancing synaptic activity with bicuculline and 4-AP led to an almost normal appearance of the ΔMyr-Jacob-GFP transfected neurons (Figure 6E). Moreover, the number of synaptic contacts was unchanged as compared to controls (Figures 6F–6H). Importantly, enhanced synaptic activity could only attenuate the ΔMyr-Jacob-GFP phenotype, but not the phosphodeficient mutant phenotype, strongly supporting the decisive role of

cytosolic nonvesicular fraction obtained after ultracentrifugation of S2 at 100,000 x *g*, P2, crude membranes; and N, purified nuclei. The S3 fraction was subsequently used for coimmunoprecipitation of α-internexin with a pan-Jacob guinea pig antibody.

(B) Dynein intermediate chain coimmunoprecipitates with α-internexin from rat brain S3 and S2 fractions. UB, unbound.

(C) Bacterially expressed recombinant MBP-Jacob-1-228 and active ERK1 were incubated with rat brain extracts containing active phosphatases for 20 min at 30°C. The presence of α-internexin fusion proteins attenuates dephosphorylation of both pJacob and pERK.

(D) α-internexin prevents dephosphorylation of pJacob, but not of pERK1, when ERK is not associated with pJacob. The phosphatase assay was performed on nitrocellulose membranes as described in Extended Experimental Procedures.

(E–H) Small hairpin RNA (shRNA) knockdown of α-internexin significantly reduces nuclear import of Jacob following 4-AP/bicuculline stimulation, but not after stimulation of extrasynaptic NMDARs. (E) and (G) Confocal images of DIV17-18 hippocampal primary neurons transfected with α-internexin shRNA knockdown and corresponding scrambled control constructs (scr). Staining with an anti-α-internexin antibody shows the efficiency of knockdown (lower panels in E and G). α-internexin and pan-Jacob (rabbit) stainings are represented as gradient lookup tables, and quantification is summarized in (F), (H), and (I). Scale bars, 10 μm. Data are represented as mean ±SEM. ***$p < 0.001$ as determined by Bonferroni corrected t tests.

See also Figures S4 and S5.

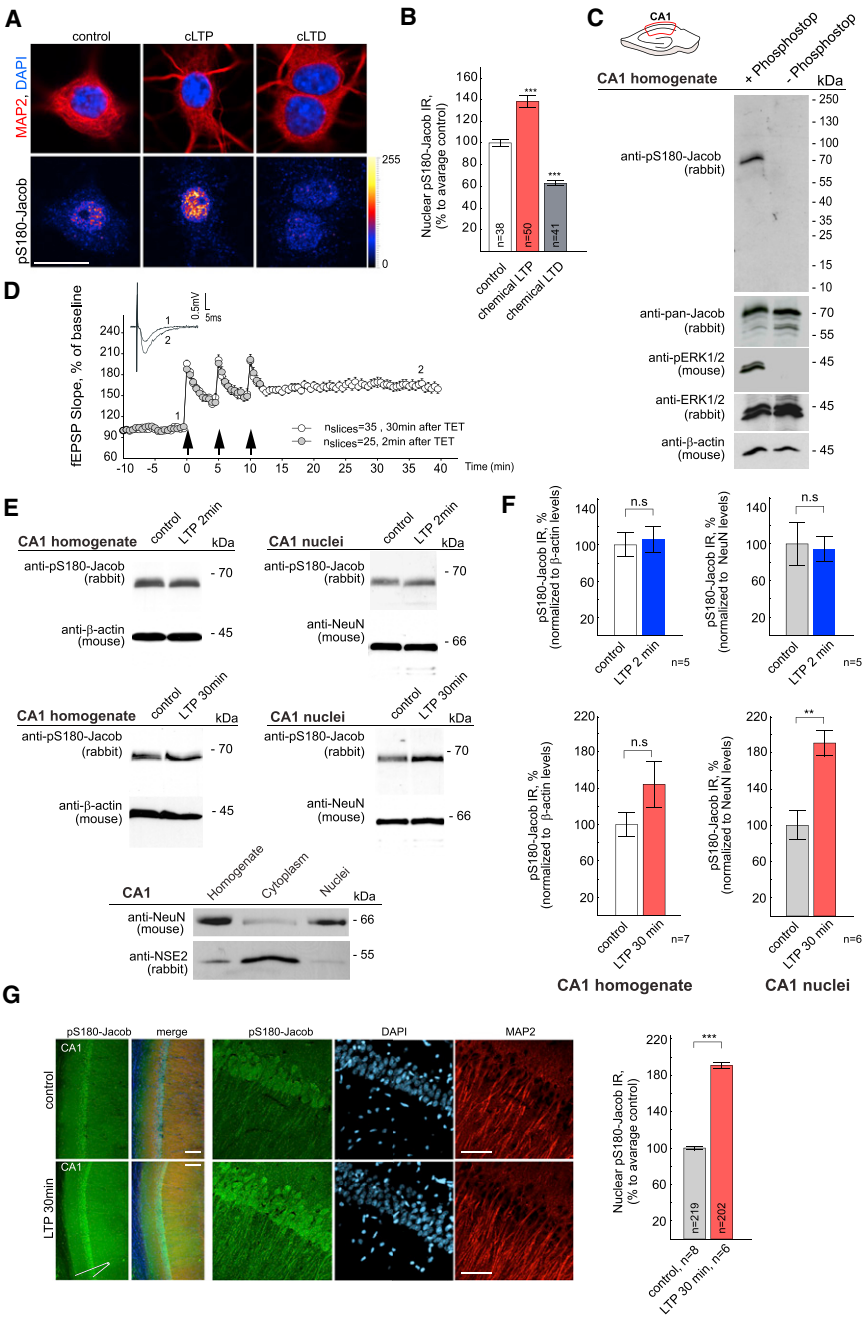


**Figure 5. NMDA-Receptor-Dependent LTP Increases Nuclear pS180-Jacob IR**

(A) Chemically induced LTP, but not LTD, increases nuclear pS180-Jacob IR in DIV17-18 hippocampal primary neurons. Scale bar, 20 μm.

(B) Intensity-based quantification of nuclear pS180-Jacob IR. Data are represented as mean ±SEM. ***$p < 0.001$ as determined by Bonferroni corrected t tests.

(C) The CA1 region from adult rat hippocampal slices was dissected and homogenized in hypotonic lysis buffer with or without phosphostop (phosphatase inhibitor). The pS180-Jacob and pERK1/2 band were only detected in samples treated with phosphatase inhibitors.

(D–F) Late LTP induced in Schaffer collateral-CA1 synapses results in a significant increase in nuclear pS180-Jacob levels 30 min after tetanization. (D) Averaged field excitatory postsynaptic potentials (fEPSP) slope values over time normalized to 10 min baseline. Insert shows representative traces of evoked fEPSP transients before and 30 min after tetanization. Arrows indicate high-frequency stimulation trains. Slices were shock frozen 2 min or 30 min after induction of LTP.

(E) pS180-Jacob levels in CA1 homogenates and in nuclear-enriched fraction. Five slices were pooled for one preparation, and a total of 25–35 slices was used for each experimental condition. Equal amounts of protein were loaded in each lane. Equal loading was controlled with β-actin (homogenates) and NeuN (nuclei) antibodies. The purity of the preparation was checked with an antibody directed against the cytoplasmic marker protein neuron-specific enolase 2 (NSE2).

(F) Quantification of pS180-Jacob IR normalized to β-actin and NeuN levels, respectively. Data are represented as mean ±SEM. **$p < 0.01$ as determined by Student's t tests.

(G) Late-LTP induced in Schaffer collateral-CA1 synapses results in increased pS180-Jacob staining intensity in nuclei of CA1 pyramidal neurons 30 min after tetanization. Stimulation (position indicated) and recording pipettes were placed in the CA1 stratum radiatum. Depicted are representative sections stained with antibodies directed against pS180-Jacob (green), MAP2 (red), and DAPI (blue) for nuclear detection. Scale bars, 100 μm in the overview and 60 μm in the magnification. Number of slices are indicated below the bar graph. Number of analyzed cells are indicated in each column. Data are represented as mean ±SEM. ***$p < 0.001$ as determined by Bonferroni corrected t tests.

Ser180 phosphorylation for the nuclear function of Jacob (Figures 6C, 6E, 6G, and 6H).

Similar results were obtained in a reporter gene assay in which we cotransfected primary hippocampal neurons with a green fluorescent protein (GFP) construct fused to the BDNF promoter and ΔMyr-S180A- or ΔMyr-S180D-Jacob mutants. The BDNF promoter contains a CRE site, and BDNF expression is a classical readout of CREB transcriptional activity (Figure 7A). Enhancing synaptic activity with bicuculline resulted in increased GFP expression (Figures 7C and 7D). Nuclear overexpression of phosphomimetic Jacob significantly enhanced GFP expression irrespective of synaptic activity, whereas transfection of the phosphodeficient construct had the opposite effect (Figures 7B and 7D).

CREB shut-off has been linked to NMDA-induced cell death and neuronal degeneration. In previous work, we found that a nuclear knockdown of Jacob attenuates NMDA-induced cell death (Dieterich et al., 2008). We therefore asked whether the presence of phosphomimetic Jacob in the nucleus might be neuroprotective. It turned out that phosphomimetic Jacob not

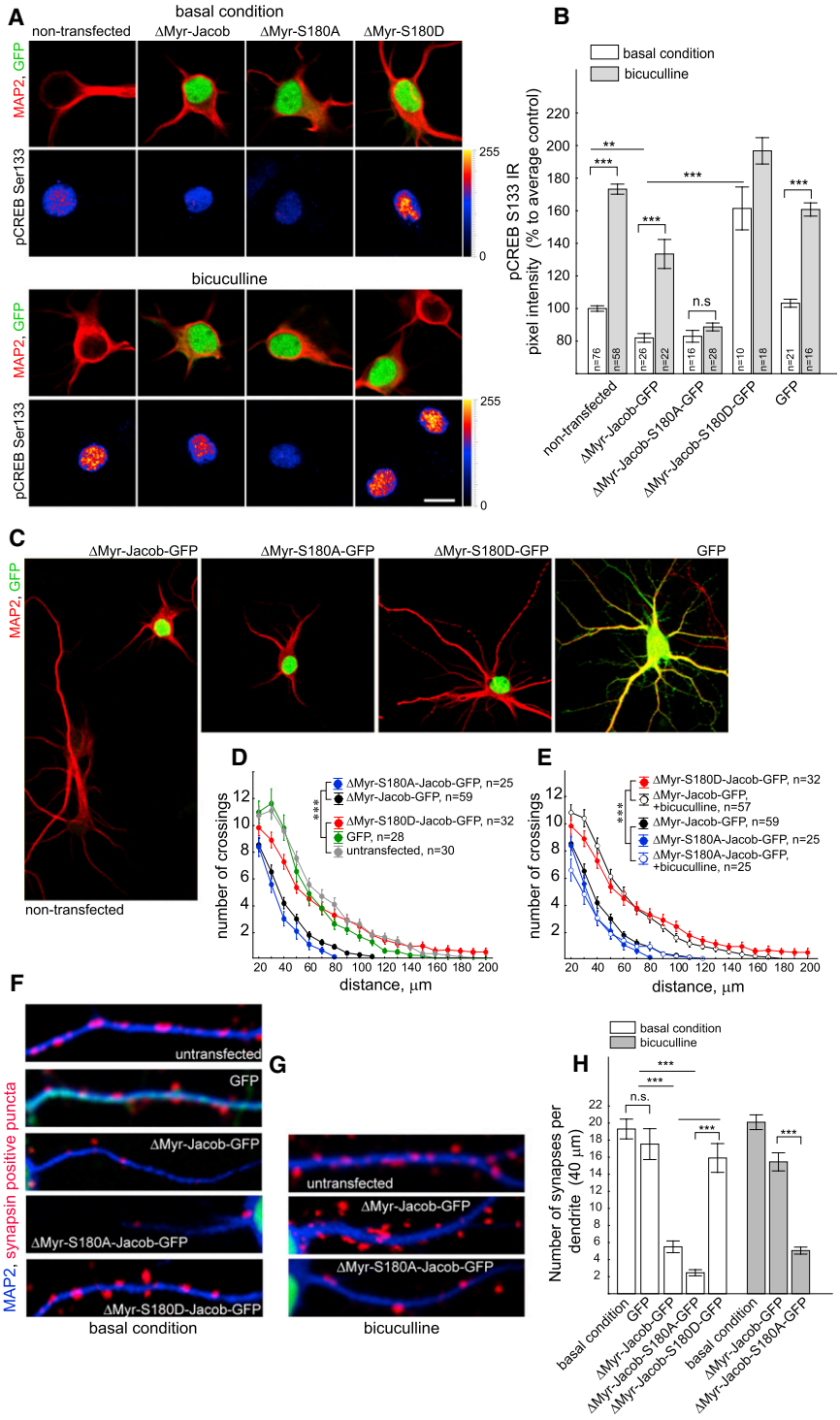


**Figure 6. Phosphomimetic (S180D) and Phosphodeficient (S180A) Jacob Regulate CREB Phosphorylation and Synapto-Dendritic Complexity in an Opposing Manner**

(A and B) Enhanced synaptic activity induced by 50 μM bicculline (12 hr) abolished CREB shut-off in neurons overexpressing nuclear ΔMyr-Jacob-GFP, but not ΔMyr-Jacob-S180A-GFP. Nuclear overexpression of phosphomimetic Jacob (ΔMyr-Jacob-S180D-GFP) results in increased pCREB IR already under basal conditions. Depicted are confocal images from hippocampal neurons transfected with ΔMyr-Jacob-GFP, ΔMyr-Jacob-S180A-GFP, or ΔMyr-S180D-Jacob-GFP and costained with antibodies against MAP2 (red) and pCREB (gradient lookup table). The PMT gain within each individual experiment was set to a value where the pCREB level after enhanced synaptic activity of NMDAR gave the highest signal without reaching saturation. Scale bar, 20 μm. The diagram (B) represents pixel intensity quantification of pCREB signals normalized to untransfected control. Data are represented as mean ±SEM. $^{**}p < 0.01$ and $^{***}p < 0.001$.

(C–F and H) Neurons overexpressing in the nucleus phosphodeficient Jacob (ΔMyr-Jacob-S180A-GFP) or Jacob that is wild-type with respect to serine 180 (ΔMyr-Jacob-GFP), but not phosphomimetic Jacob (ΔMyr-Jacob-S180D-GFP), exhibit a reduced synapto-dendritic complexity under resting conditions.

(D and E) Overexpression of ΔMyr-Jacob-GFP (black circles) and ΔMyr-Jacob-S180A-GFP (blue circles), but not ΔMyr-S180D-Jacob-GFP (red circles), results in reduced dendritic complexity. The phenotype of ΔMyr-Jacob-GFP, but not ΔMyr-Jacob-S180A-GFP, overexpression can be significantly attenuated by bath application of 50 μM bicuculline (black open circles and blue open circles, respectively) following transfection. The complexity of the dendritic tree was analyzed by Sholl analysis based on MAP2 staining.

(F–H) The synaptic phenotype of ΔMyr-Jacob-GFP, but not of ΔMyr-JacobS180A-GFP, overexpression can be reduced by bath application of 50 μM bicuculline following transfection. (C), (F), and (G) depict confocal images of hippocampal neurons overexpressing Jacob mutants or GFP costained with anti-MAP2 and anti-synapsin antibodies (in F and G). Scale bar, 40 μm. (F and G) Dendrites from cells kept under resting conditions or 21 hr in the presence of bicuculline, respectively. MAP2 staining is indicated in blue; red spots represent presynaptic terminals visualized with anti-synapsin antibody staining. Data are represented as mean ±SEM. $^{***}p < 0.001$ as determined by Bonferroni corrected t tests.

See also Figure S6.

only fostered the phosphorylation of CREB but also significantly reduced apoptosis even in cultures treated with 100 μM NMDA for 5 min (Figures 7E and 7F). Of note, the neuroprotection conferred by overexpression of the phosphomimetic Jacob mutant was still significant 12 hr after the insult, despite the nuclear import of endogenous nonphosphorylated Jacob under these conditions.

The decisive role of ERK phosphorylation for the nuclear function of Jacob is further underscored by the finding that viral expression of ΔMyr-S180D-Jacob, but not of ΔMyr-S180A-Jacob,

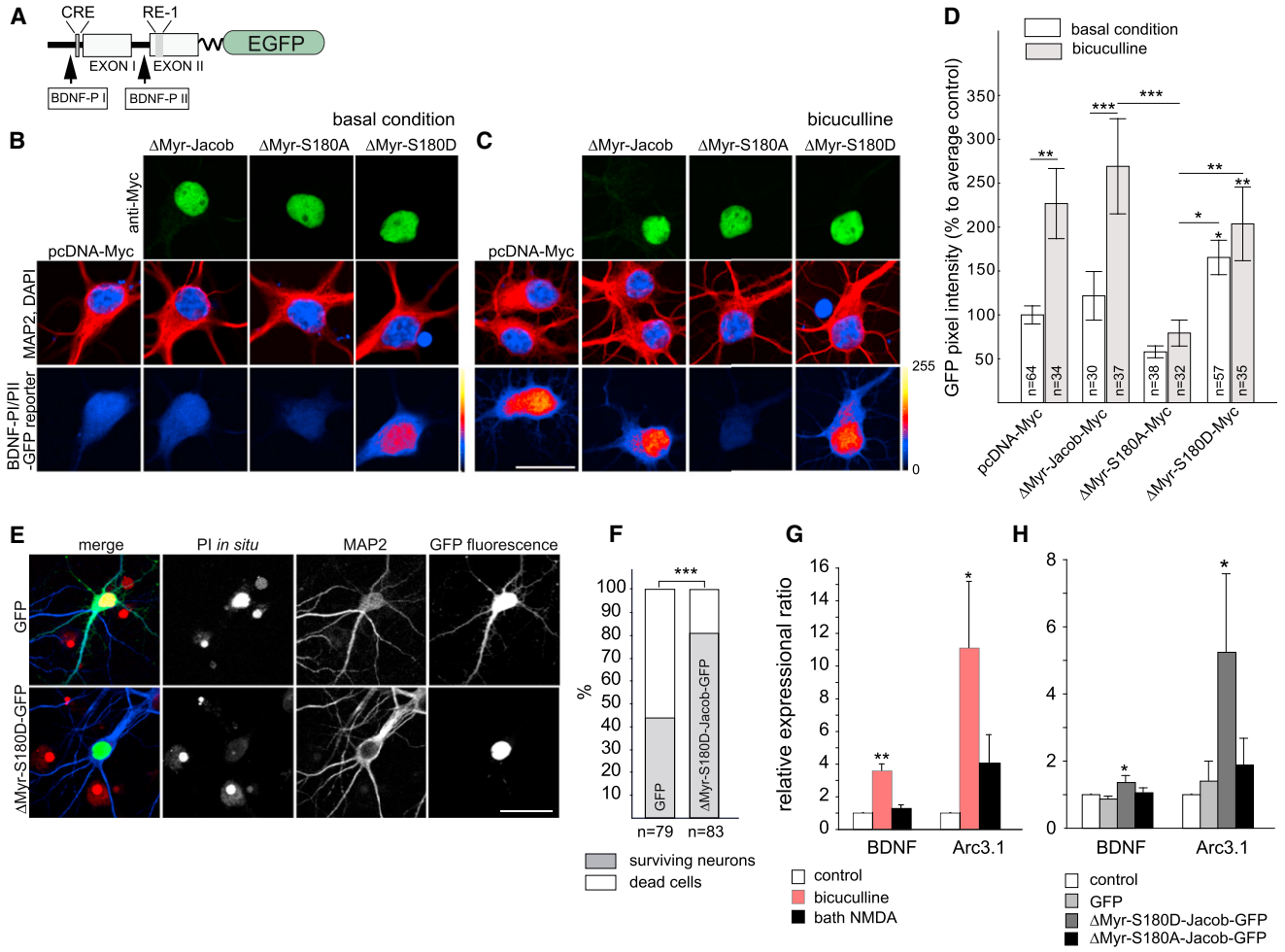


**Figure 7. Phosphomimetic S180D and Phosphodeficient S180A Jacob Regulate BDNF Gene Transcription, Cell Death, and Cell Survival in an Opposing Manner**

(A–D) Effect of nuclear Jacob overexpression (ΔMyr-Jacob-Myc, phosphomimetic ΔMyr-S180D-Jacob-Myc, or phosphodeficient ΔMyr-S180A-Jacob-Myc mutants) in a BDNF-promoter reporter gene expression system. The lower panel depicts the GFP expression (shown in a gradient lookup table) under basal conditions and in cultures kept in 50 μM bicuculline (B and C). Scale bar, 20 μm.

(D) Intensity-based quantification measured as mean gray value in arbitrary units and normalized to controls. Data are represented as mean ±SEM. *$p < 0.05$, **$p < 0.01$, and ***$p < 0.001$ as determined by Bonferroni corrected t tests.

(E and F) Phosphomimetic Jacob promotes cell survival. Hippocampal neurons were transfected with ΔMyr-Jacob-S180D-GFP or GFP and treated for 5 min with 100 μM bath NMDA at DIV12 followed by 12 hr washout. Neuronal degeneration was monitored by quantification of propidium iodide uptake. Data are represented as mean ±SEM. ***$p < 0.001$ as determined nonparametric Cochran Q-test.

(G) Application of 50 μM bicculline (6 hr) leads to elevated mRNA levels of BDNF and Arg/Arc3.1 as evidenced by quantitative real-time PCR.

(H) Nuclear overexpression of phosphomimetic ΔMyr-Jacob-S180D-GFP in primary neurons kept under basal conditions leads to an increased expression of BDNF and arc/arg3.1. Values in (G) and (H) were normalized to Hprt1. Data are represented as mean ±SEM. *$p < 0.05$ and **$p < 0.01$ in (G) and (H) as determined by Bonferroni corrected t tests.

induces significantly higher transcript levels of the neuronal-plasticity-related genes BDNF and Arc/Arg3.1, resembling an expression pattern seen after enhancing synaptic NMDAR activity in cortical primary cultures (Figures 7G and 7H). Moreover, the gene expression induced by ΔMyr-S180D-Jacob feeds back to synaptic function. Patch-clamp experiments revealed that neurons expressing this construct in the nucleus exhibit a higher mEPSC amplitude, but not mEPSC frequency, as compared to control cells (Figures S6C–S6E). Thus, the gene expression induced by nuclear pS180-Jacob provides a plasticity signal that enhances synaptic efficacy.

## DISCUSSION

Here, we provide evidence for a long-distance signaling pathway that encodes the synaptic and extrasynaptic localization of activated NMDARs in the nucleus. Following synaptic NMDAR activation and, in contrast to extrasynaptic NMDAR, Jacob

carries an ERK phosphorylation signature that defines it as a synapto-nuclear protein messenger, designating the synaptic localization of NMDARs that drove its nuclear translocation. Although different signaling mechanisms downstream of both types of NMDARs have been previously described, this study identifies a mechanism that differentiates between these pathways for long-distance signaling. In a physiological context, the pJacob-pERK-α-internexin association provides a new molecular mechanism for a synapto-nuclear protein messenger signalosome involved in long-distance signaling and deciphering of synaptic versus extrasynaptic dendritic signals.

The scenario developed from this and previous studies (Dieterich et al., 2008; Kindler et al., 2009; Behnisch et al., 2011) suggests that, irrespective of receptor localization, NMDAR activation results in the nuclear import of Jacob (Figure S7). Neuronal importin-α can directly associate with NMDARs (Jeffrey et al., 2009), and the translocation process requires the binding of Jacob to importin-α under both conditions, synaptic or extrasynaptic NMDAR activation (Figure S7). In the case of a synaptic origin of the NMDAR signal, pERK will associate with Jacob and phosphorylate Ser180 at synaptic sites, which, in turn, is a prerequisite for Jacob to leave the synapse (Figure S7). It can be tacitly assumed that the activation of ERK at synaptic sites either requires the RasGRF- or the αCamKII-Ras-MEK pathway (Krapivinsky et al., 2003; El Gaamouch et al., 2012). It was suggested that RasGRF1 directly binds to the GluN2B subunit and induces LTD via activation of p38MAP-kinase, whereas RasGRF2 only associates with the GluN2A subunit and is involved in the induction of LTP via activation of ERK (Li et al., 2006). However, the vast majority of synaptic NMDARs are probably triheteromeric (Rauner and Köhr, 2011), and the idea that GluN2A and GluN2B receptors are differentially involved in LTP and LTD induction (Liu et al., 2004) has been challenged (Morishita et al., 2007).

At first glance, it appears unlikely that the phosphorylation signal can be preserved during transport from distal dendrites to the nucleus due to the high phosphatase activity in neurons. However, Perlson et al. (2005) could show that retrograde transport of ERK in axons requires association with importin-β and the molecular motor dynein and that the concomitant binding of vimentin hinders the dephosphorylation of pERK. In analogy to this scenario, we found that C-terminal fragments of α-internexin prevent the dephosphorylation of pJacob and pERK in a trimeric complex. In addition, we observed that this complex is very stable. Knockdown of α-internexin indeed blocked the nuclear import of Jacob after stimulation of synaptic NMDARs, but not extrasynaptic NMDARs. We therefore propose that, analogous to axons, a nonvesicular transport mechanism along microtubuli exists in dendrites, requiring neuronal importins, dynein, and a filament protein that functions as an adaptor to prevent dephosphorylation and the loss of the kinase signal (Figure S7).

Our data suggest that Jacob predominantly exists in a pERK-bound form after synaptic NMDAR activation because the non-phosphorylated kinase binds with considerably lower affinity. However, it should be stressed that Jacob binding only provides a link to active retrograde synapto-nuclear transport for a subfraction of pERK1/2. Facilitated diffusion, rather than active transport, has been postulated to underlie the nuclear accumulation of pERK1/2 in response to enhanced neuronal activity (Wiegert et al., 2007). Also the higher abundance of ERK1/2 precludes a major role of Jacob in the regulation of nuclear ERK1/2 trafficking. In addition, a larger proportion of the synapto-dendritic Jacob pool remains stationary after enhanced synaptic NMDAR activity. The assembly of the proposed pJacob/pERK signalosome at synaptic sites and the details of the transport processes await further clarification. At present, it is unclear if and how this complex is disassembled in the nucleus and why Jacob's trafficking from synapses to the nucleus, but not from extrasynaptic sites, requires ERK phosphorylation.

Nuclear Jacob mediates either cell death or survival (Figure S7). This function seems to be associated with the transcriptional activity of CREB. Jacob is found in complexes that contain DNA and RNA polymerase II (Dieterich et al., 2008), and it can directly associate with CREB (R.K. and M.R.K., unpublished data). This raises the possibility that Jacob might bring signaling components to the CREB complex. It is widely believed that CaMKIV mediates fast CREB phosphorylation at Ser133, whereas ERK1/2 promote CREB phosphorylation in a slower, but more persistent manner (Hardingham et al., 2001; Wu et al., 2001). Our data show that pJacob, pERK, and α-internexin are present in a very stable trimeric complex. It is tempting to speculate that pJacob may possess a scaffolding function for the localization of pERK in nuclear signaling complexes containing CREB after stimulation of synaptic NMDARs. Another yet-to-be-identified mechanism will, in turn, induce CREB shut-off following nuclear import after extrasynaptic NMDAR activation.

The latter function of Jacob suggests that it might be involved in cellular processes associated with extrasynaptic NMDAR activity, including brain ischemia and Huntington's disease (Okamoto et al., 2009; Milnerwood et al., 2010; Tu et al., 2010). However, recent studies also suggest a physiological role of extrasynaptic NMDARs in augmenting synaptic signaling (Harris and Pettit, 2008) as well as in the regulation of homeostatic plasticity (Wang et al., 2011). Glutamate spillover following high-frequency stimulation might stimulate extrasynaptic NMDARs under physiological conditions and elicit nuclear import of Jacob. This is of interest because Jacob can eventually be phosphorylated in various subcellular compartments, and the extrasynaptic versus synaptic pathway might be concomitantly active, leading to a dynamic equilibrium of phosphorylated and nonphosphorylated Jacob complexes translocating into the nucleus (Figure S7). A caveat of the present study is that it lacks proof in vivo. Future work using transgenic mouse models should address this issue.

## EXPERIMENTAL PROCEDURES

### Expression Constructs, Antibodies, and Primary Cell Culture

A list of all constructs, antibodies, information about the preparation of viruses, immunocytochemical stainings, and live-imaging experiments can be found in Extended Experimental Procedures (Tables S1 and S2).

### Subcellular Brain Fractionation and Biochemical Assays

Preparation of PSD-enriched fractions was done as described previously (Dieterich et al., 2008). Pull-down assays were carried out as described previously (Mikhaylova et al., 2009). Further information about the expression and

purification of recombinant proteins and interaction assays can be found in Extended Experimental Procedures.

### Biophysical Experiments, Quantitative Real-Time PCR, and Electrophysiology

A detailed description of electrophysiological recordings, messenger RNA (mRNA) experiments, mass spectrometry, and SPR interaction studies is included in Extended Experimental Procedures.

## SUPPLEMENTAL INFORMATION

Supplemental Information includes Extended Experimental Procedures, seven figures, and two tables and can be found with this article online at http://dx.doi.org/10.1016/j.cell.2013.02.002.

## ACKNOWLEDGMENTS

We want to thank C. Borutzki, M. Marunde, and S. Hochmuth for technical assistance; N. Ziv for helpful discussion; J. Lindquist for proofreading: M. Tsuda, A. Fejtova, D. Ivanova, J. Wiedemann, and U. Thomas for providing constructs; M. Hupe for assistance in α-internexin experiments; A.C. Lehmann for help with cloning; and Y. Chen and P. Yuan Xiang for assistance in electrophysiology. This work was supported by the DFG (SFB 779 TPB8 to M.R.K.; TPZ to T.K. and M.N.; SFB854 TP7 to M.R.K.; TP4 to M.N.; TP8 to E.D.G.; GRK1167 and Kr1879/3-1 to M.R.K.); DIP grant to E.D.G. and M.R.K.; EU FP7 MC-ITN NPlast to M.R.K.; European Regional Development Fund (ERDF 2007–2013); Vorhaben: CBBS to A.K. and C.S.; NSFC 31271197 to T.B.; and the Schram Foundation to M.R.K. M.M. is the recipient of a European Molecular Biology Organization (EMBO) long-term fellowship (EMBO ALTF 884-2011) and is supported by Marie Curie Actions (EMBOCOFUND2010, GA-2010-267146).

Received: May 22, 2012
Revised: December 11, 2012
Accepted: February 1, 2013
Published: February 28, 2013

## REFERENCES

Alberini, C.M. (2009). Transcription factors in long-term memory and synaptic plasticity. Physiol. Rev. *89*, 121–145.

Behnisch, T., Yuanxiang, P., Bethge, P., Parvez, S., Chen, Y., Yu, J., Karpova, A., Frey, J.U., Mikhaylova, M., and Kreutz, M.R. (2011). Nuclear translocation of jacob in hippocampal neurons after stimuli inducing long-term potentiation but not long-term depression. PLoS ONE *6*, e17276.

Benson, D.L., Mandell, J.W., Shaw, G., and Banker, G. (1996). Compartmentation of alpha-internexin and neurofilament triplet proteins in cultured hippocampal neurons. J. Neurocytol. *25*, 181–196.

Deisseroth, K., Bito, H., and Tsien, R.W. (1996). Signaling from synapse to nucleus: postsynaptic CREB phosphorylation during multiple forms of hippocampal synaptic plasticity. Neuron *16*, 89–101.

Dieterich, D.C., Karpova, A., Mikhaylova, M., Zdobnova, I., König, I., Landwehr, M., Kreutz, M., Smalla, K.H., Richter, K., Landgraf, P., et al. (2008). Caldendrin-Jacob: a protein liaison that couples NMDA receptor signalling to the nucleus. PLoS Biol. *6*, e34.

El Gaamouch, F., Buisson, A., Moustié, O., Lemieux, M., Labrecque, S., Bontempi, B., De Koninck, P., and Nicole, O. (2012). Interaction between αCaMKII and GluN2B controls ERK-dependent plasticity. J. Neurosci. *32*, 10767–10779.

Flavell, S.W., and Greenberg, M.E. (2008). Signaling mechanisms linking neuronal activity to gene expression and plasticity of the nervous system. Annu. Rev. Neurosci. *31*, 563–590.

Hanz, S., Perlson, E., Willis, D., Zheng, J.Q., Massarwa, R., Huerta, J.J., Koltzenburg, M., Kohler, M., van-Minnen, J., Twiss, J.L., and Fainzilber, M. (2003). Axoplasmic importins enable retrograde injury signaling in lesioned nerve. Neuron *40*, 1095–1104.

Hardingham, G.E., and Bading, H. (2010). Synaptic versus extrasynaptic NMDA receptor signalling: implications for neurodegenerative disorders. Nat. Rev. Neurosci. *11*, 682–696.

Hardingham, G.E., Arnold, F.J., and Bading, H. (2001). A calcium microdomain near NMDA receptors: on switch for ERK-dependent synapse-to-nucleus communication. Nat. Neurosci. *4*, 565–566.

Harris, A.Z., and Pettit, D.L. (2008). Recruiting extrasynaptic NMDA receptors augments synaptic signaling. J. Neurophysiol. *99*, 524–533.

Ivanov, A., Pellegrino, C., Rama, S., Dumalska, I., Salyha, Y., Ben-Ari, Y., and Medina, I. (2006). Opposing role of synaptic and extrasynaptic NMDA receptors in regulation of the extracellular signal-regulated kinases (ERK) activity in cultured rat hippocampal neurons. J. Physiol. *572*, 789–798.

Jeffrey, R.A., Ch'ng, T.H., O'Dell, T.J., and Martin, K.C. (2009). Activity-dependent anchoring of importin alpha at the synapse involves regulated binding to the cytoplasmic tail of the NR1-1a subunit of the NMDA receptor. J. Neurosci. *29*, 15613–15620.

Jordan, B.A., and Kreutz, M.R. (2009). Nucleocytoplasmic protein shuttling: the direct route in synapse-to-nucleus signaling. Trends Neurosci. *32*, 392–401.

Kim, M.J., Dunah, A.W., Wang, Y.T., and Sheng, M. (2005). Differential roles of NR2A- and NR2B-containing NMDA receptors in Ras-ERK signaling and AMPA receptor trafficking. Neuron *46*, 745–760.

Kindler, S., Dieterich, D.C., Schütt, J., Sahin, J., Karpova, A., Mikhaylova, M., Schob, C., Gundelfinger, E.D., Kreienkamp, H.J., and Kreutz, M.R. (2009). Dendritic mRNA targeting of Jacob and N-methyl-d-aspartate-induced nuclear translocation after calpain-mediated proteolysis. J. Biol. Chem. *284*, 25431–25440.

Köhr, G. (2006). NMDA receptor function: subunit composition versus spatial distribution. Cell Tissue Res. *326*, 439–446.

Krapivinsky, G., Krapivinsky, L., Manasian, Y., Ivanov, A., Tyzio, R., Pellegrino, C., Ben-Ari, Y., Clapham, D.E., and Medina, I. (2003). The NMDA receptor is coupled to the ERK pathway by a direct interaction between NR2B and RasGRF1. Neuron *40*, 775–784.

Li, S., Tian, X., Hartley, D.M., and Feig, L.A. (2006). Distinct roles for Ras-guanine nucleotide-releasing factor 1 (Ras-GRF1) and Ras-GRF2 in the induction of long-term potentiation and long-term depression. J. Neurosci. *26*, 1721–1729.

Liu, L., Wong, T.P., Pozza, M.F., Lingenhoehl, K., Wang, Y., Sheng, M., Auberson, Y.P., and Wang, Y.T. (2004). Role of NMDA receptor subtypes in governing the direction of hippocampal synaptic plasticity. Science *304*, 1021–1024.

Mikhaylova, M., Reddy, P.P., Munsch, T., Landgraf, P., Suman, S.K., Smalla, K.H., Gundelfinger, E.D., Sharma, Y., and Kreutz, M.R. (2009). Calneurons provide a calcium threshold for trans-Golgi network to plasma membrane trafficking. Proc. Natl. Acad. Sci. USA *106*, 9093–9098.

Milnerwood, A.J., Gladding, C.M., Pouladi, M.A., Kaufman, A.M., Hines, R.M., Boyd, J.D., Ko, R.W., Vasuta, O.C., Graham, R.K., Hayden, M.R., et al. (2010). Early increase in extrasynaptic NMDA receptor signaling and expression contributes to phenotype onset in Huntington's disease mice. Neuron *65*, 178–190.

Morishita, W., Lu, W., Smith, G.B., Nicoll, R.A., Bear, M.F., and Malenka, R.C. (2007). Activation of NR2B-containing NMDA receptors is not required for NMDA receptor-dependent long-term depression. Neuropharmacology *52*, 71–76.

Okamoto, S., Pouladi, M.A., Talantova, M., Yao, D., Xia, P., Ehrnhoefer, D.E., Zaidi, R., Clemente, A., Kaul, M., Graham, R.K., et al. (2009). Balance between synaptic versus extrasynaptic NMDA receptor activity influences inclusions and neurotoxicity of mutant huntingtin. Nat. Med. *15*, 1407–1413.

Papadia, S., Soriano, F.X., Léveillé, F., Martel, M.A., Dakin, K.A., Hansen, H.H., Kaindl, A., Sifringer, M., Fowler, J., Stefovska, V., et al. (2008). Synaptic NMDA receptor activity boosts intrinsic antioxidant defenses. Nat. Neurosci. *11*, 476–487.

Perlson, E., Hanz, S., Ben-Yaakov, K., Segal-Ruder, Y., Seger, R., and Fainzilber, M. (2005). Vimentin-dependent spatial translocation of an activated MAP kinase in injured nerve. Neuron *45*, 715–726.

Perlson, E., Michaelevski, I., Kowalsman, N., Ben-Yaakov, K., Shaked, M., Seger, R., Eisenstein, M., and Fainzilber, M. (2006). Vimentin binding to phosphorylated Erk sterically hinders enzymatic dephosphorylation of the kinase. J. Mol. Biol. *364*, 938–944.

Rauner, C., and Köhr, G. (2011). Triheteromeric NR1/NR2A/NR2B receptors constitute the major N-methyl-D-aspartate receptor population in adult hippocampal synapses. J. Biol. Chem. *286*, 7558–7566.

Rönicke, R., Mikhaylova, M., Rönicke, S., Meinhardt, J., Schröder, U.H., Fändrich, M., Reiser, G., Kreutz, M.R., and Reymann, K.G. (2011). Early neuronal dysfunction by amyloid β oligomers depends on activation of NR2B-containing NMDA receptors. Neurobiol. Aging *32*, 2219–2228.

Thomas, G.M., and Huganir, R.L. (2004). MAPK cascade signalling and synaptic plasticity. Nat. Rev. Neurosci. *5*, 173–183.

Thompson, K.R., Otis, K.O., Chen, D.Y., Zhao, Y., O'Dell, T.J., and Martin, K.C. (2004). Synapse to nucleus signaling during long-term synaptic plasticity; a role for the classical active nuclear import pathway. Neuron *44*, 997–1009.

Tu, W., Xu, X., Peng, L., Zhong, X., Zhang, W., Soundarapandian, M.M., Balel, C., Wang, M., Jia, N., Zhang, W., et al. (2010). DAPK1 interaction with NMDA receptor NR2B subunits mediates brain damage in stroke. Cell *140*, 222–234.

Wang, C.C., Held, R.G., Chang, S.C., Yang, L., Delpire, E., Ghosh, A., and Hall, B.J. (2011). A critical role for GluN2B-containing NMDA receptors in cortical development and function. Neuron *72*, 789–805.

Wiegert, J.S., Bengtson, C.P., and Bading, H. (2007). Diffusion and not active transport underlies and limits ERK1/2 synapse-to-nucleus signaling in hippocampal neurons. J. Biol. Chem. *282*, 29621–29633.

Wu, G.Y., Deisseroth, K., and Tsien, R.W. (2001). Activity-dependent CREB phosphorylation: convergence of a fast, sensitive calmodulin kinase pathway and a slow, less sensitive mitogen-activated protein kinase pathway. Proc. Natl. Acad. Sci. USA *98*, 2808–2813.

Yuan, A., Rao, M.V., Sasaki, T., Chen, Y., Kumar, A., Veeranna, Liem, R.K., Eyer, J., Peterson, A.C., Julien, J.P., and Nixon, R.A. (2006). Alpha-internexin is structurally and functionally associated with the neurofilament triplet proteins in the mature CNS. J. Neurosci. *26*, 10006–10019.

Zhang, S.J., Steijaert, M.N., Lau, D., Schütz, G., Delucinge-Vivier, C., Descombes, P., and Bading, H. (2007). Decoding NMDA receptor signaling: identification of genomic programs specifying neuronal survival and death. Neuron *53*, 549–562.

Zhang, S.J., Buchthal, B., Lau, D., Hayer, S., Dick, O., Schwaninger, M., Veltkamp, R., Zou, M., Weiss, U., and Bading, H. (2011). A signaling cascade of nuclear calcium-CREB-ATF3 activated by synaptic NMDA receptors defines a gene repression module that protects against extrasynaptic NMDA receptor-induced neuronal cell death and ischemic brain damage. J. Neurosci. *31*, 4978–4990.